2009

Effect of Water Transport on the Production of Hydrogen and Sulfuric Acid in a PEM Electrolyzer

John A. Staser
University of South Carolina - Columbia

John W. Weidner
University of South Carolina - Columbia, weidner@engr.sc.edu

Publication Info

Journal of the Electrochemical Society, 2009, pages B16-B21.

Publisher's link: http://dx.doi.org/10.1149/1.3001923
DOI: 10.1149/1.3001923

Journal of The Electrochemical Society, **156** (1) B16-B21 (2009)
0013-4651/2008/156(1)/B16/6/$23.00 © The Electrochemical Society

Effect of Water Transport on the Production of Hydrogen and Sulfuric Acid in a PEM Electrolyzer

John A. Staser* **and John W. Weidner****,z**

Center for Electrochemical Engineering, Department of Chemical Engineering, University of South Carolina, Columbia, South Carolina 29208, USA

The thermochemical cycle involving the interconversion between sulfur dioxide and sulfuric acid is a promising method for efficient, large-scale production of hydrogen. A key step in the process is the oxidation of sulfur dioxide to sulfuric acid in an electrolyzer. Gaseous SO_2 fed to a proton exchange membrane (PEM) electrolyzer was previously investigated and was shown to be a promising system for the electrolysis step. A critical factor in the performance of this gas-fed electrolyzer is the management of water since it: (*i*) is needed as a reactant, (*ii*) determines the product sulfuric acid concentration, (*iii*) affects SO_2 crossover rate, and (*iv*) serves to hydrate the membrane. Therefore, we present a coupled mathematical and experimental study on the effect of water on the production of sulfuric acid in a gas-phase PEM electrolyzer. The model is shown to successfully predict the concentration of sulfuric acid as a function of temperature, current density, pressure differential across the membrane, and membrane thickness.
 [DOI: 10.1149/1.3001923]

Manuscript submitted August 27, 2008; revised manuscript received September 24, 2008. Published October 30, 2008.

To use hydrogen as a renewable energy carrier on a large scale, a method must be developed that provides efficient production of clean hydrogen. The methods existing today for large-scale production of hydrogen typically involve hydrocarbon reforming of natural gas or coal gasification. Not only is hydrocarbon reforming nonrenewable, but the hydrogen produced is often contaminated with trace impurities, such as carbon monoxide.[1-4] Electrolysis of water has the advantage in that the hydrogen produced is highly pure, and there are zero emissions from the process. However, low-temperature electrolysis is relatively inefficient due to the low thermal to electrical energy efficiency of current power plants ($<30\%$) and the efficiency of the alkaline electrolyzer ($\sim 40\%$).[5,6] Hence, the overall efficiency of low-temperature electrolysis can be $<10\%$.[6] Low-temperature electrolysis has advantages for small, distributed hydrogen generation, but the low efficiency eliminates it as a practical choice for large-scale hydrogen production.

High-temperature electrolysis, especially when coupled with advanced nuclear reactors expected to meet thermal to electric efficiencies of $>70\%$,[1] are expected to approach overall efficiencies of 50% if the electrolysis efficiency is 95%; if the electrolysis efficiency is lower (i.e., 75%), the overall efficiency is $<40\%$.[7] Two issues remain, however, that make the future of this technology uncertain. The operating current densities are low (i.e., 0.2 A/cm^2 at 1.25 V and 830°C),[8] and much progress must be made in the development of materials suitable for long-term operation at high temperatures in corrosive environments.

Overall, direct water electrolysis has distinct disadvantages in efficiency and required materials. A recent Department of Energy (DOE) Energy Information Administration reported that electrolyzers can potentially reach efficiencies of 60–63%, but the inefficiencies in electricity generation for this process to supply the energy for the electrolysis step drastically reduce the overall process efficiency.[9]

Thermochemical cycles have recently received attention as an alternative to high-temperature electrolysis for large-scale, efficient production of hydrogen. The leading candidates for the thermochemical water-splitting cycles are the sulfur-based processes.[10-18] These processes require energy at high temperature (~ 850°C) for one of the steps, which makes them ideal candidates to be coupled with next-generation nuclear reactors or solar-thermal towers. In these sulfur-based thermochemical cycles, the high-temperature step involves the decomposition of H_2SO_4 to produce oxygen and sulfur dioxide via the following reaction

$$H_2SO_4 \rightarrow SO_2 + \tfrac{1}{2}O_2 + H_2O \quad [1]$$

The sulfur dioxide that is generated from Reaction 1 is converted back to H_2SO_4, with the production of hydrogen balancing the reaction. In the sulfur-iodine process, this is accomplished by reacting SO_2 with iodine to produce H_2SO_4 and HI. The HI is then converted to I_2 and H_2 in a decomposition reactor. The difficulty arises when separating HI from the water and iodine before decomposition to hydrogen. In addition to this energy-intensive separation step, serious material problems are encountered because of the corrosive nature of HI.[10,11]

In an alternative process, Westinghouse Corporation developed the Hybrid-Sulfur (HyS) process that completely eliminates iodine from the process.[13,14] Westinghouse dissolved SO_2 in sulfuric acid, and oxidized it at the anode according to the reaction

$$SO_2 + 2H_2O \rightarrow H_2SO_4 + 2H^+ + 2e^- \quad E^\circ = 0.17 \text{ V vs SHE} \quad [2]$$

where SHE is the standard hydrogen electrode.

The protons produced at the anode migrated through the porous separator and reduced to hydrogen at the cathode. The reaction at the water-fed cathode was the hydrogen evolution reaction

$$2H^+ + 2e^- \rightarrow H_2 \quad E^\circ = 0 \text{ V vs SHE} \quad [3]$$

Overall, the hybrid-sulfur electrolyzer consumes sulfur dioxide and water and produces sulfuric acid at the anode and hydrogen at the cathode. The overall electrolyzer reaction is given as

$$SO_2 + 2H_2O \rightarrow H_2SO_4 + H_2 \quad [4]$$

Combining Reactions 1 and 4, the overall HyS process is water and energy (heat and electricity) converted to hydrogen and oxygen.

In addition, a potential parasitic reaction may occur at the cathode due to the crossover of SO_2 through the membrane that results in the reduction of SO_2 to sulfur at the cathode

$$SO_2 + 4e^- \rightarrow S + O_2 \quad [5]$$

Reaction 5 consumes current that would otherwise be used for the production of hydrogen, produces oxygen in the hydrogen stream, and produces sulfur deposits that may increase cell resistance over time. The extent to which Reaction 5 affects the hybrid-sulfur process is not known.

It has been estimated that, with an advanced nuclear plant capable of achieving 45% thermal-to-electric conversion efficiency, the overall HyS process efficiency would be 10% greater than that of water electrolysis.[17] This estimate allowed for an electrolysis efficiency of 68%, as opposed to the optimistic 95% value used by others.[7,17]

* Electrochemical Society Student Member.
** Electrochemical Society Active Member.
z E-mail: weidner@engr.sc.edu

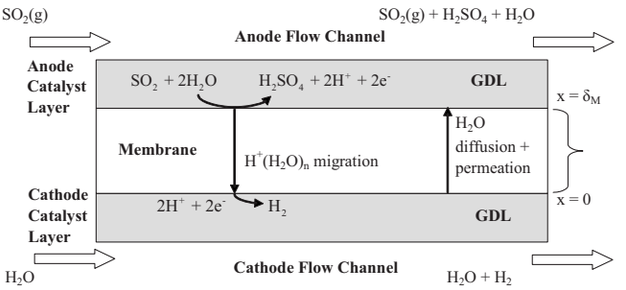

Figure 1. Schematic of the model system under consideration. Dry SO_2 gas and liquid water are fed to the anode and cathode, respectively. Water diffuses across the Nafion membrane from the cathode to the anode due to a gradient in the water activity. Water also moves to the anode with a pressure gradient and is transported back to the cathode via electro-osmotic drag.

To further increase the current density and lower the operating voltage, we modified the HyS process by feeding pure gaseous SO_2 (as opposed to SO_2 dissolved in sulfuric acid) to the anode of a proton exchange membrane (PEM) electrolyzer.[15,16] We achieved 0.2 and 0.5 A/cm^2 at 0.62 and 0.71 V, respectively.[16] In that report, we showed that Pt loading in the electrode has no effect on electrolyzer performance, but that temperature and membrane thickness strongly influenced the performance. We attributed the effect of temperature and membrane thickness to a lower membrane resistance and better water management for thinner membranes at higher temperatures.

In our gas-phase process, the water required for Reaction 2 is supplied by the cathode via the membrane (see Fig. 1). The rate of water transport across the membrane is a difference between water diffusing toward the anode and electro-osmotic drag toward the cathode. The flux of water can be further influenced by hydraulic permeation due to a pressure differential across the membrane. Hence, in this paper we develop a mathematical model, in conjunction with experimental data, to predict water transport due to the combined effects of diffusion, permeation, and electro-osmotic drag. The net flux of water is used to determine the amount and concentration of sulfuric acid as a function of membrane thickness, temperature, current density, and pressure differential across the membrane. The sulfuric acid concentration is a critical factor in the overall efficiency of the HyS process because more energy is required to heat diluted sulfuric acid for the decomposition step.

Experimental

The experimental setup was similar to that reported in our previous paper.[16] The electrolyzer cell was the standard 10 cm^2 cell purchased from Fuel Cell Technologies, Inc. This cell was modified so that the electrolyzer reactants and products were passed through Kynar plates instead of the standard aluminum end plates to avoid corrosion by H_2SO_4. The membrane was Nafion of three thicknesses: N117 (7 mil extrusion cast film), N115 (5 mil extrusion cast film), and N212 (2 mil dispersion cast film). Carbon cloth gas diffusion layers from E-TEK were placed between the membrane electrode assembly and the carbon flow channels. The electrodes were Pt-black with 1.5 mg/cm^2 for N212 and N115, and were Pt-carbon with 1.0 mg/cm^2 Pt for N117. As shown previously,[16] the type and loading of Pt had a negligible effect on electrolyzer performance.

The baseline operating conditions for the electrolyzer were 80°C, the anode pressure was P_a = 101 kPa, and the cathode pressure was P_c = 700 kPa. Hence, the pressure differential across the membrane $\Delta P = (P_c - P_a)$ was ~600 kPa. The anode pressure was maintained at 101 kPa for all experiments reported here, and the cathode pressure was maintained by a globe valve placed at the exit of the electrolyzer cathode. The conversion rate of SO_2 was 20%. Our previous work showed a negligible effect of conversion on electrolyzer performance.[16]

The exiting sulfuric acid concentration was measured with a pH meter. It has been shown that H_2SO_4 does not fully dissociate at concentrations of >1 M.[19]

The results obtained from the pH meter were compared to titrations using 1 N NaOH. The pH meter was accurately calibrated to the titration experiments over the range of sulfuric acid concentrations reported here.

Table I. Parameters used in the simulations.

		Ref.
Diffusion coefficient of water ($D_{w,F}$)	Eq. 7 and 8	17
Density of membrane (ρ_M)	2.0 g/cm^3	18
Molecular weight of membrane (M_M)	1100 g/mol	18
Thickness of membrane (δ_M)	Variable	[a]
Total pressure (P)	Variable	[a]
Membrane pressure differential (ΔP)	Variable	[a]

[a] Measured.

Model Development

The electrolyzer operates as shown in Fig. 1. Gaseous SO_2 fed to the electrolyzer reacts with water at the anode via Reaction 2, forming H_2SO_4 (i.e., sulfuric acid) and producing protons that migrate to the cathode. The rate of H_2SO_4 production is constant at each current density and determined by Faraday's law. Because the current density is the same at every point on the electrode, the production rate of H_2SO_4, the water flux, and, hence, the concentration of sulfuric acid is uniform throughout the electrolyzer. Therefore, the model is one-dimensional in the x direction (through the membrane). The water flux across the membrane is given by

$$N_w = \frac{\rho_M}{M_M \delta_M} \int_{\lambda_a}^{\lambda_c} D_{w,F}\, d\lambda - \frac{\xi \lambda_a i_{H_2SO_4}}{\lambda_c F} + \frac{P_M}{\delta_M}(P_c - P_a) \quad [6]$$

The first term on the right-hand side of Eq. 6 is the diffusion rate of water across the membrane, and it is a function of temperature. This term is identical to that used previously to predict the water transport during the production of hydrogen and chlorine from anhydrous HCl in a PEM electrolyzer.[20] The second term is the flux through the membrane due to the electro-osmotic drag, and it is also the same as that used previously (ξ = 2.5).[20] The third term is the water transport rate due to a pressure differential across the membrane. The parameter P_M is the water permeability of the membrane.

The expression for $D_{w,F}$ was given previously as[21]

$$D_{w,F} = A_1 \lambda (1 + e^{-0.28\lambda}) \exp\left[\frac{-2436}{T}\right] \quad (\text{for } 0 < \lambda \leq 3) \quad [7]$$

$$D_{w,F} = A_2 \lambda (1 + 161 e^{-\lambda}) \exp\left[\frac{-2436}{T}\right] \quad (\text{for } 3 < \lambda \leq 17) \quad [8]$$

The pre-exponential factors A_1 and A_2 depend on the membrane type but not the thickness. As demonstrated previously,[20] the water content at the cathode, λ_c, is constant and equal to the water content of the membrane in contact with pure water, which was measured to be 22 and 18 at 30 and 80°C, respectively.[21,22] The water content at the anode, λ_a, is determined by the water activity in the following[23]

$$\lambda_a = 0.043 + 17.81 a_w - 39.85 a_w^2 + 36.0 a_w^3 \quad [9]$$

where a_w is the water activity given by the following water and H_2SO_4 balance

$$a_w = \left(\frac{N_w - \frac{i_{H_2SO_4}}{F}}{N_w} \right) \quad [10]$$

A list of model parameters is given in Table I.

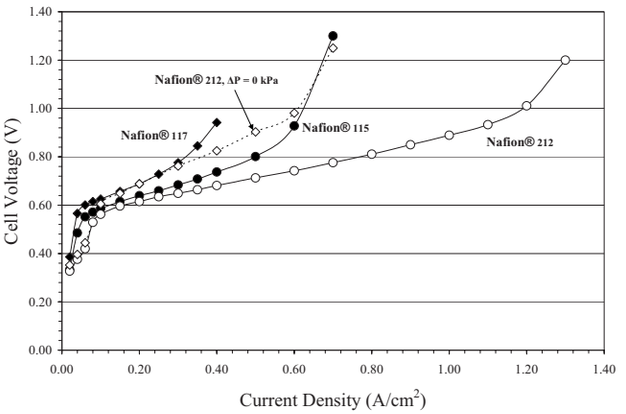

Figure 2. Polarization curve data for Nafion 117, 115, and 212 electrolyzers. The water transport to the anode influences cell voltage. Water flux is higher for thinner membranes and increases with the pressure differential across the membrane. Unless noted differently in the graph, ΔP was 600 kPa. The cell temperature was 80°C.

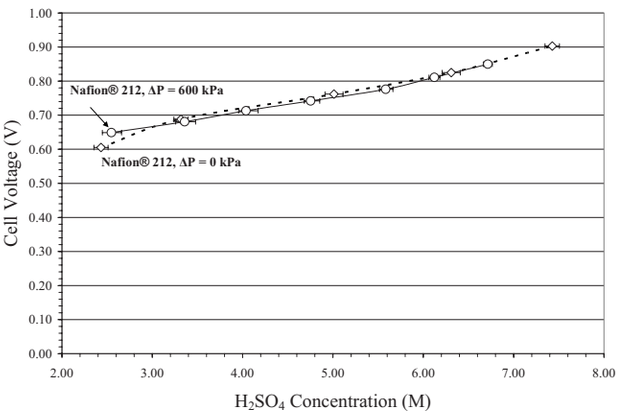

Figure 3. Comparison of cell voltage for Nafion 212 for $\Delta P = 0$ and 600 kPa as a function of sulfuric acid concentration. Because the two cell voltages at the same sulfuric acid concentrations are equal, the increased cell voltage for the $\Delta P = 0$ kPa electrolyzer in Fig. 2 is due to the increased sulfuric acid concentration. The cell temperature was 80°C.

Results and Discussion

The polarization curves for the electrolyzers with Nafion 117, 115, and 212 run with a pressure differential ($\Delta P = P_c - P_a$) of 600 kPa are given in Fig. 2, and are the same results published previously.[16] Also included in this figure are the results from the Nafion 212 membrane run with zero pressure differential. The symbols are experimental data and the lines are smooth curve fits to the data. As expected, the cell voltage decreases as the membrane thickness decreases. The results from the N212 electrolyzer run with a zero pressure differential further illustrate the effect of water flux on the cell voltage. The data in Fig. 2 show that the cell voltage increases as the pressure differential decreases ($\sim$0.20 V at 0.5 A/cm^2). The electrolyzer also could not be operated at current densities of $>$0.6 A/cm^2 with a zero pressure differential. The cell voltages for N212 operated with a zero pressure differential are comparable to those of N117 operated with a 600 kPa pressure differential.

It was previously concluded that the differences in the polarization (*V-I*) curves for the three different membranes were due to different membrane resistances at moderate current densities.[16] It was speculated that the voltage was not sensitive to water transport as long as sufficient water crossed the membrane to sustain Reaction 2. However, the N212 membrane at $\Delta P = 0$ kPa more closely matches the N117 membrane at $\Delta P = 600$ kPa, even though the resistance of the membranes is not a function of pressure differential. The pressure differential does affect the water flux or, therefore, the sulfuric acid concentration. Hence, the effect of water transport on the cell voltage must be related to the concentration of sulfuric acid formed at the anode.

This is clear when the voltage is plotted vs sulfuric acid concentration for the two different N212 cases, as shown in Fig. 3. Again, the symbols are experimental data with errors in the measurement of sulfuric acid taken into account and the lines are smooth curve fits to the data. These two curves are virtually identical; the voltage penalty for producing H_2 at 700 kPa is $\sim$0.025 V. Therefore, a key factor influencing the cell voltage is the sulfuric acid concentration. As a result, accurately predicting, and ultimately controlling, water transport as a function of design (e.g., membrane thickness and type) and operating (e.g., temperature, pressure differential, current) parameters is critical for the efficient operation of the electrolyzer.

To accurately predict sulfuric acid concentration as a function of the pressure differential, the variables P_M in Eq. 6 and A_1 and A_2 in Eq. 7 and 8 must be determined for each membrane as a function of pressure differential. The molar flux of water across the membrane at 80°C is given in Fig. 4 as a function of the pressure differential across the membrane. The cell was run with N_2 as the carrier gas at the anode and at open-circuit voltage. The symbols are experimental data, and the lines are least-squares fits to these data. As expected, the water flux increases with increasing pressure differential. This experiment was repeated at 50 and 65°C, and no measurable difference in the water flux was measured. The resulting permeability value for Nafion was $P_M = 1.1 \times 10^{-10}$ mol/cm s/kPa.

The variables A_1 and A_2 were determined from the ΔP = 600 kPa case for Nafion 212 to correspond to the experimental data at 0.30 A/cm^2. The values of A_1 and A_2 were found to be 2.60×10^{-3} and 3.96×10^{-4} cm^2/s, respectively, and were not a function of thickness or temperature.

After the values of P_M and A_1 and A_2 were determined, it was possible to employ the model over the entire range of operating current densities, pressure differentials, temperature and membrane thickness, and provide insight into the operation of the electrolyzer without any adjustable parameters. Figure 5 shows data (symbols) and model simulations (lines) for the production of sulfuric acid for Nafion 212 electrolyzer at 80°C and $\Delta P = 600$ kPa. The errors in measuring the sulfuric acid production rate are more pronounced at low current density, where the production rate is low, but are negli-

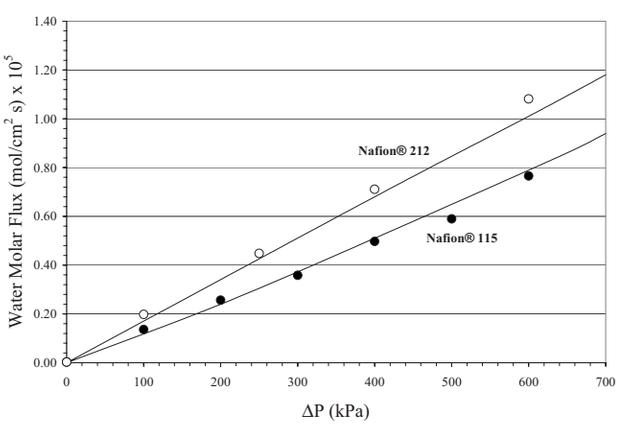

Figure 4. Experimental data (symbols) at open circuit for the effect of pressure differential on water flux across Nafion 115 and 212. Nitrogen was fed to the anode at 100 sccm, and water was fed to the cathode. The cell temperature was 80°C. The nitrogen pressure was maintained at 101 kPa, and the pressure difference across the membrane was controlled by a globe valve on the cathode side. The model was fit to the data to determine P_M in Eq. 6.

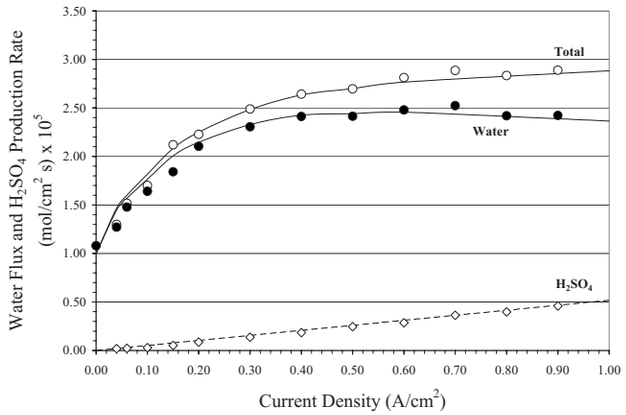

Figure 5. Contribution of water and H_2SO_4 to the total volumetric flow rate of the Nafion 212 electrolyzer. The points are experimental data and the lines are model predictions. After 0.7 A/cm^2, the water flow rate begins to decrease due to electro-osmotic drag. The total volumetric flow rate continues to increase due to the increased production of H_2SO_4. The cell temperature was 80°C and ΔP was 600 kPa.

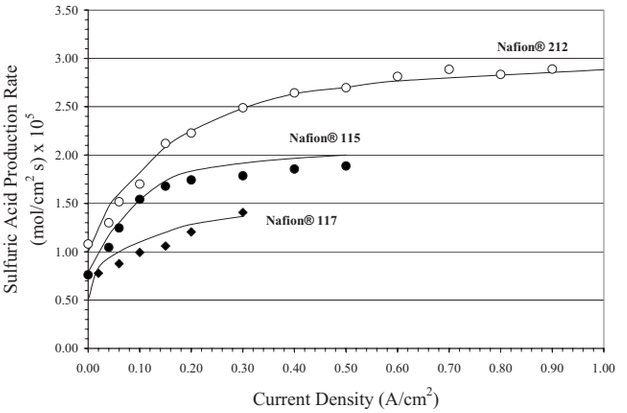

Figure 7. Experimental data (symbols) and model predictions (lines) for sulfuric acid production rate as a function of current density for the three different membrane thicknesses. The model shows good agreement with the experimental data, with a prediction that the total molar flow rate increases with increasing current density. The cell temperature was 80°C and ΔP was 600 kPa.

gible. The sulfuric acid is separated into the H_2SO_4 and water. These results confirm that the electrolyzer is not limited by water reaching the anode to participate in Reaction 2. There is excess water crossing the membrane to participate in the reaction. In fact, the amount of water available for the reaction increases with current density.

It has also been suggested that acid transport across the membrane may exist.[24,25] This phenomenon has been studied and found to be negligible; it has been determined that the flux of formic acid through Nafion 117 was 2.03×10^{-8} mol/cm^2 s at 25°C, vs a methanol flux of 3–6 $\times 10^{-8}$ mol/cm^2 s.[24] In fact, Nafion has been investigated as a means to concentrate sulfuric acid for the thermochemical cycles; feeding sulfuric acid to one side of a Nafion membrane resulted in water flux through the membrane sufficient enough to result in a highly concentrated sulfuric acid stream.[25] Our experimental data confirms that we detect >95% of the H_2SO_4 at the anode predicted by Faraday's law.

To better understand why the amount of water crossing the membrane increases with current, the individual contributions to the total water flux shown in Fig. 5 are plotted in Fig. 6. The experimental data for the total water flux (symbols) have been plotted along with the model simulations (lines). At low current densities, the molar flux of water increases with increasing current density due to an

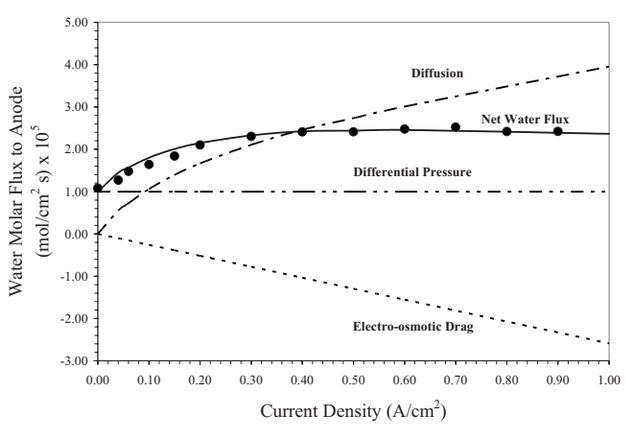

Figure 6. Contributions of diffusional flux and electro-osmotic drag to the net water diffusion and pressure effects work to offset the electro-osmotic drag effect. The symbols are data, and the lines are model predictions. The cell temperature was 80°C and ΔP was 600 kPa.

increase in the amount of H_2SO_4 produced at the anode. The presence of H_2SO_4 reduces the water activity and leads to an increase in concentration-driven diffusion from the cathode. As the current density increases, however, this phenomenon is increasingly offset by the electro-osmotic drag, which pulls water back across the membrane to the cathode. A situation then exists in which the flux due to diffusion competes with electro-osmotic drag. The pressure-driven flux is the same over all current densities.

The experimental data (symbols) and model simulations (lines) for the production rate of sulfuric acid as a function of current and membrane thickness (Nafion 117, 115, and 212) are shown in Fig. 7. As expected, the production rate of sulfuric acid increases with current because water transport and H_2SO_4 production increase. It also increases with decreasing membrane thickness because more water is transported across the thinner membranes at each current. The sulfuric acid production rates at 0.5 A/cm^2 are 1.89×10^{-5} and 2.75×10^{-5} mol/cm^2 s for Nafion 115 and 212 electrolyzers, respectively. Nafion 117 cannot operate at this current density. For Nafion 117 at 0.3 A/cm^2, the production rate of sulfuric acid is 1.41×10^{-5} mol/cm^2 s.

Because the sulfuric acid concentration affects cell voltage, it is desirable to study sulfuric acid concentration as a function of membrane thickness, current density, and pressure differential. The experimental concentration data (symbols) and model simulations (lines) for ΔP = 600 kPa are given in Fig. 8. Again, there is good agreement between the two values; the data more closely agree with the model at current densities of >0.2 A/cm^2 because of the difficulty in accurately measuring the pH of the sulfuric acid produced at very low current densities. At 0.5 A/cm^2, the experimental concentrations are 5.88 and 4.33 M for Nafion 115 and Nafion 212 electrolyzers, respectively. The model predictions for these two electrolyzers are 5.72 and 4.46 M. For the Nafion 117 electrolyzer at 0.3 A/cm^2, the experimental and model predictions for the H_2SO_4 concentration are 5.14 and 5.15 M, respectively. As expected, the sulfuric acid concentration decreases as membrane thickness decreases. The increased water flux through the thinner membranes dilutes the sulfuric acid.

The sulfuric acid concentration for Nafion 212 with ΔP = 0 kPa are also presented in Fig. 8. These sulfuric acid concentrations are very close to those of Nafion 117 with ΔP = 600 kPa. This result is expected when one considers Fig. 2, in which it was shown that the cell voltages were very similar for Nafion 212 at ΔP = 0 kPa and Nafion 117 at ΔP = 600 kPa. Sulfuric acid concentration can be closely correlated to cell voltage.

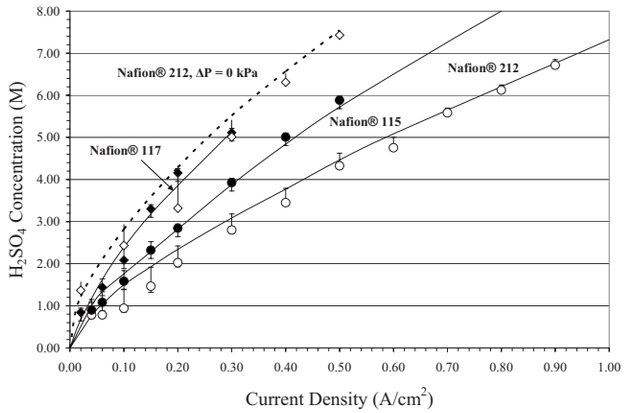

Figure 8. Experimental data (symbols) and model predictions (lines) for the concentration of H_2SO_4 produced in the electrolyzer. The sulfuric acid concentration increases with current density and membrane thickness, and decreases with an increase in the pressure differential. Unless noted differently in the graph, the cell temperature was 80°C and ΔP was 600 kPa.

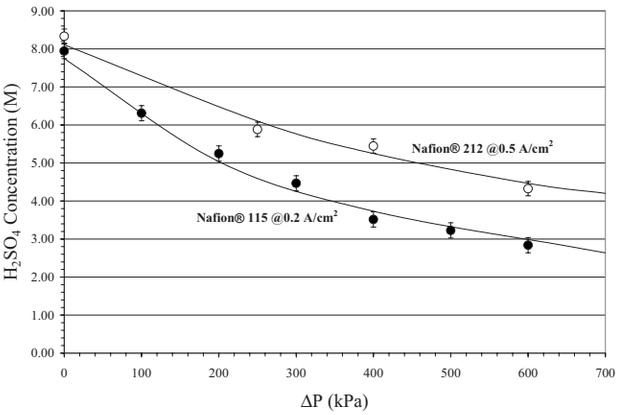

Figure 10. Experimental data (symbols) and model predictions (lines) for sulfuric acid concentration as a function of pressure for Nafion 115 and 212. The sulfuric acid concentration decreases with ΔP due to the increase in water flux to the anode. The cell temperature was 80°C and the anode pressure was 101 kPa. The water pressure at the cathode was controlled by a globe valve.

Because it was shown in Fig. 8 that the pressure differential influences the sulfuric acid concentration, one would expect that the sulfuric acid production rate would change with the pressure differential. This is indeed what is observed in Fig. 9 for sulfuric acid production rate in the N115 electrolyzer operated at 0.2 A/cm^2 and the N212 electrolyzer operated at 0.5 A/cm^2. As expected, the sulfuric acid production rate increases with pressure differential. Again, the model simulations (lines) closely follow the experimental data (symbols). For example, at ΔP = 400 kPa the experimental sulfuric acid production rate for N115 at 0.2 A/cm^2 is 1.37 $\times$ 10^{-5} mol/cm^2 s, and the model prediction is 1.33 $\times$ 10^{-5} mol/cm^2 s. For N212 at 0.5 A/cm^2, the experimental rate is 2.15 $\times$ 10^{-5} mol/cm^2 s and the model prediction is 2.22 $\times$ 10^{-5} mol/cm^2 s.

We have already seen in Fig. 8 and 9 that increasing the pressure differential decreases the sulfuric acid concentration and increases the sulfuric acid production rate. Continuing this investigation, the sulfuric acid concentration for the N115 and N212 electrolyzers are presented as a function of pressure differential in Fig. 10. At ΔP = 400 kPa, the experimental (symbol) sulfuric acid concentration for Nafion 115 at 0.2 A/cm^2 is 3.52 M and the model prediction (line) is 3.73 M. For Nafion 212 at 0.5 A/cm^2, the experimental sulfuric acid concentration is 5.45 M and the model prediction is 5.25 M. The Nafion 212 was operated at 0.5 A/cm^2 vs 0.2 A/cm^2 for N115 in Fig. 9 and 10 simply because Nafion 115 could not reach 0.5 A/cm^2 at ΔP = 0 kPa.

The sulfuric acid production rate data (symbols) for Nafion 212 at two different temperatures (50 and 80°C) and two different pressure differentials (0 and 600 kPa) are presented in Fig. 11, along with the model simulations (lines). The highest rate is observed at 80°C and ΔP = 600 kPa due to the increased rate of water diffusion at high temperature and the increased pressure-driven flux at a high pressure differential. At 50°C and ΔP = 600 kPa, the experimental sulfuric acid production rate at 0.5 A/cm^2 is 2.12 $\times$ 10^{-5} mol/cm^2 s and the model prediction is 2.00 $\times$ 10^{-5} mol/cm^2 s. At 80°C and ΔP = 0 kPa, the experimental sulfuric acid production rate at 0.5 A/cm^2 is 1.35 $\times$ 10^{-5} mol/cm^2 s and the model prediction is 1.38 $\times$ 10^{-5} mol/cm^2 s.

From Fig. 11, we can see that increasing the pressure differential has a greater effect on sulfuric acid production rate than increasing the temperature. That is, the sulfuric acid production rate increases more with pressure differential than with temperature. This is due to

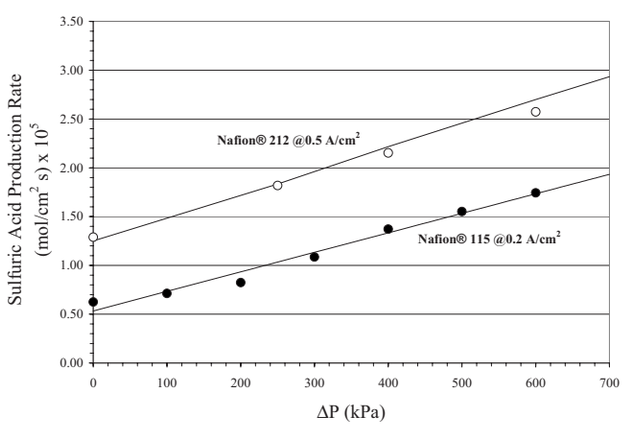

Figure 9. Experimental data (symbols) and model predictions (lines) for sulfuric acid production as a function of ΔP for Nafion 115 and 212. Sulfuric acid concentration increases with ΔP due to the increase in water flux to the anode. The cell temperature was 80°C. The pressure gradient was controlled by a globe valve.

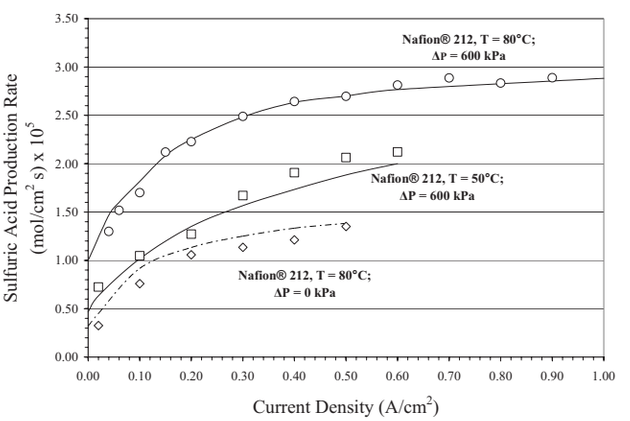

Figure 11. Experimental data (symbols) and model predictions (lines) for sulfuric acid production rate for Nafion 212 at different temperatures and differential pressures. The sulfuric acid flux increases with temperature and pressure gradient.

the greater increase in pressure-driven flux of water through the membrane with increasing pressure differential than water diffusion due to an increase in the temperature.

Conclusions

We have developed a mathematical model, in conjunction with experimental data, to predict water transport in a PEM electrolyzer fed with gaseous SO_2. We predicted the combined effects of diffusion, permeation, and electro-osmotic drag and show how these influence cell performance. We now understand how water transport affects the sulfuric acid concentration, which influences the cell voltage. There is a trade-off between low voltages (large water transport) and high sulfuric acid concentrations (low water transport) in that a higher sulfuric acid concentration is desired for downstream decomposition, but concentrated sulfuric acid increases the cell voltage and hence the power required to drive the electrolyzer. A full, system-level optimization is needed to determine the desired electrolyzer operating conditions. The model developed here can aid in this optimization. The model also reveals how the water transport rate can be manipulated by independently varying design (e.g., membrane thickness) and operating conditions (e.g., temperature, current, pressure differential).

Acknowledgment

The authors thank the U.S. DOE for funding this work (grant no. DE-FC07-06ID14752).

University of South Carolina assisted in meeting the publication costs of this article.

List of Symbols

A_1,A_2	pre-exponential factor in Eq. 7 and 8, respectively, cm^2/s
a_w	activity of water
$D_{w,F}$	Fickian diffusion coefficient of water, cm^2/s
$i_{H_2SO_4}$	current density, A/cm^2
M_M	molecular weight of membrane, g/mol
N_w	flux of water, mol/cm^2s
ΔP	pressure differential across the membrane, kPa
P_M	membrane permeability, mol/cm s/kPa
T	temperature, K
x	distance perpendicular to the membrane, cm

Greek

δ_M	thickness of the catalyst coated membrane, cm
λ_a	water content of the membrane on the anode side
λ_c	water content of the membrane on the cathode side
ρM	density of Nafion, g/cm^3

References

1. M. A. Rosen, *Int. J. Hydrogen Energy*, **21**, 349 (1996).
2. M. A. Rosen and D. S. Scott, *Int. J. Hydrogen Energy*, **23**, 653 (1998).
3. M. A. Rosen, *Int. J. Hydrogen Energy*, **20**, 547 (1995).
4. S. Z. Baykara, *Int. J. Hydrogen Energy*, **29**, 1451 (2004).
5. E. Varkaraki, N. Lymberopoulos, E. Zoulias, D. Guichardot, and G. Poli, *Int. J. Hydrogen Energy*, **32**, 1589 (2007).
6. M. B. Gorensek, Paper presented at the AIChE Spring 2005 Meeting, Session 73, April 11, 2005.
7. Y. Shin, W. Park, J. Chang, and J. Park, *Int. J. Hydrogen Energy*, **32**, 1486 (2007).
8. J. S. Herring, J. E. O'Brien, C. M. Stoots, G. L. Hawkes, J. J. Hartvigsen, and M. Shahnam, *Int. J. Hydrogen Energy*, **32**, 440 (2007).
9. Department of Energy (DOE) Energy Information Administration, Hydrogen Use, Petroleum Consumption and Carbon Dioxide Emissions, Washington, DC (2008).
10. Nuclear Hydrogen R&D Plan Draft, Department of Energy, Office of Nuclear Energy, Science and Technology, 2004.
11. Nuclear Hydrogen Initiative: Ten Year Program Plan, Office of Advanced Nuclear Research, DOE Office of Nuclear Energy, Science and Technology, March 2005.
12. A. Hauch, S. H. Jensen, S. Ramousse, and M. Mogensen, *J. Electrochem. Soc.*, **153**, A1741 (2006).
13. P. W. Lu, E. R. Garcia, and R. L. Ammon, *J. Appl. Electrochem.*, **11**, 347 (1981).
14. P. W. Lu and R. L. Ammon, *J. Electrochem. Soc.*, **127**, 2610 (1980).
15. P. Sivasubramanian, R. P. Ramasamy, F. J. Freire, C. E. Holland, and J. W. Weidner, *Int. J. Hydrogen Energy*, **32**, 463 (2007).
16. J. A. Staser, R. P. Ramasamy, P. Sivasubramanian, and J. W. Weidner, *Electrochem. Solid-State Lett.*, **10**, E17 (2007).
17. M. B. Gorensek and W. A. Summers, *Int. J. Hydrogen Energy*, In press. [DOI: /10.1016/j.ijhydene.2008.06.49].
18. F. Jomard, J. P. Feraud, and J. P. Caire, *Int. J. Hydrogen Energy*, **33**, 1142 (2008).
19. P. Batamack and J. Fraissard, *Catal. Lett.*, **49**, 129 (1997).
20. S. Motupally, A. J. Becker, and J. W. Weidner, *J. Electrochem. Soc.*, **149**, D63 (2002).
21. S. Motupally, A. J. Becker, and J. W. Weidner, *J. Electrochem. Soc.*, **147**, 1371 (2000).
22. T. E. Springer, T. A. Zawodzinski, and S. Gottesfeld, *J. Electrochem. Soc.*, **138**, 2334 (1991).
23. T. A. Zawodzinski, T. E. Springer, J. Davey, R. Jestel, C. Lopez, J. Valerio, and S. Gottesfeld, *J. Electrochem. Soc.*, **140**, 1981 (1993).
24. Y. W. Rhee, S. Y. Ha, and R. I. Masel, *J. Power Sources*, **117**, 35 (2003).
25. F. F. Stewart and C. J. Orme, Annual Meeting of the American Institute of Chemical Engineers, Nov. 2006.